W Morocco shortening during the Central Atlantic early post-rift

Fernández-Blanco, D.[1], Gouiza, M.[2], Klaver, J.[3], Brautigam, K.[4], Kluge, C.[1] and Bertotti, G.[1]

[1] TU Delft University, Faculty of Civil Engineering and Geosciences, Delft, Netherlands - corresponding author: Corresponding author contact data: Email geo.david.fernandez@gmail.com // OrcID 0000-0002-5326-9164 // Telf 0034 658 023314

[2] University of Leeds, School of Earth and Environment, Leeds, England, UK

[3] RWTH Aachen University, Structural Geology, Tectonics and Geomechanics, Aachen, Germany

[4] Vrije Universiteit Amsterdam, Tectonics and Structural Geology Department, Amsterdam, Netherlands

Abstract

The early post-rift phase of the Moroccan Atlantic margin is characterized by km-scale exhumation and erosion of its eastwards continental domains, coupled with an excessive subsidence seawards. We investigate the tectonic processes behind such Late Jurassic-Early Cretaceous crustal exhumation event, which remains unclear given that it took place significantly later than lithospheric breakup but prior to the Atlas/Alpine contraction. We study the Jbel Amsittene Anticline, which is ideally located on the coastal plain of the Atlantic rifted margin of Morocco and classically considered to develop by Late Cretaceous halokinesis and Neogene Atlas contraction. Our structural analysis indicates that this anticline is a fault propagation fold verging north that formed by active tectonics during Atlantic post-rift times, with a Triassic salt acting as a detachment plane. The anticline grew by NNW-SSE to NNE-SSW shortening as indicated by syn-tectonic wedges, regional kinematic indicators and structures in the Upper Jurassic to Lower Cretaceous rocks. It was further deformed and tightened during the Cenozoic, presumably in relation to the Atlas/Alpine contraction, as shown by km-scale tête-plongeante geometry at the axis of the anticline. Contrarily to observations in other sites of the Moroccan Atlantic margin, this paper favours a "tectonics-drives-salt" over a "salt-drives-tectonics" model, and points to factors other than small-cell mantle convection affecting the evolution of the rifted margin.

KEYWORDS: exhumation; W Africa; continental margin; shortening tectonics; Amsittene; anticline

1 Introduction

The evolution of the Atlantic rifted margin in Morocco is marked by a period of abnormal and excessive subsidence during the Late Jurassic-Early Cretaceous (Gouiza 2011; Bertotti and Gouiza 2012). This early post-rift subsidence affected the distal deep basins, the continental shelf and the proximal coastal basins of the Atlantic margin, and was coeval with km-scale exhumation and erosion of large domains in the east (Gouiza et al., 2017; Ghorbal et al. 2008; Ghorbal 2009; Saddiqi et al. 2009; Oukassou et al. 2013; Leprêtre et al. 2015). The tectonics of the exhumation event are still unclear, as it took place 30 to 50 My after lithospheric breakup between Morocco and Nova Scotia (Klitgord and Schouten 1986; Sahabi et al. 2004) and prior to the Atlas/Alpine shortening, which gave rise to the Atlas and the Rif mountain belts (Frizon de Lamotte et al. 1991, 2008; Laville and Piqué 1992). Attempts to link the Late Jurassic-Early Cretaceous exhumation in the east to the coeval subsidence in the west have shown the existence of contemporaneous NE-SW to NNE-SSW shortening that might have driven both upward and downward vertical movements along the margin (Gouiza 2011; Bertotti and Gouiza 2012). Similarly to other passive continental margins, where comparable movements have been detected (Japsen and Chalmers 2000; Japsen et al. 2006, 2009; Peulvast et al. 2008; Bonow et al. 2009), these anomalous vertical movements must be driven by regional tectonic processes, yet unknown. In this contribution, we provide field evidences from the Essaouira Basin to shed light on these tectonic processes.

The Essaouira Basin is located on the coastal plain of the Atlantic rifted margin of Morocco, bounded to the E and NE by the exhumed Palaeozoic basement highs of Massif Ancien of Marrakech and the Jebilet, respectively. The Essaouira Basin is thus an ideal location to investigate the tectonic processes responsible for the aforementioned vertical movements (Fig. 1, Fig. 2). Most of the compressional structures observed in the Essaouira Basin are attributed to the Alpine shortening events leading to the uplift of the Atlas Belt (Hafid et al. 2006; Hafid 2000; Ellouz et al. 2003). Thickness changes observed in Upper Jurassic to Upper Cretaceous rocks are interpreted as resulting from synsedimentary halokinesis (Hafid et al. 2006; Hafid 2000). However, recent studies show that many contractional structures developed during the Late Jurassic-

Early Cretaceous in the western High Atlas and surroundings (Gouiza 2011; Bertotti and Gouiza 2012; Benvenuti et al. 2017). The Jbel Amsittene Anticline, located in the central western part of the Essaouira Basin, is one of several comparable structures within the western Moroccan basins thought to be formed by salt diapirism from the Late Cretaceous onwards (Piqué et al. 1998; Hafid 2000; Le Roy and Piqué 2001). In this work, we carry out a structural analysis of the Jbel Amsittene based on field observations and structural modeling to investigate the tectonics of its formation and its relationship with the regional vertical movements recorded along the Atlantic margin.

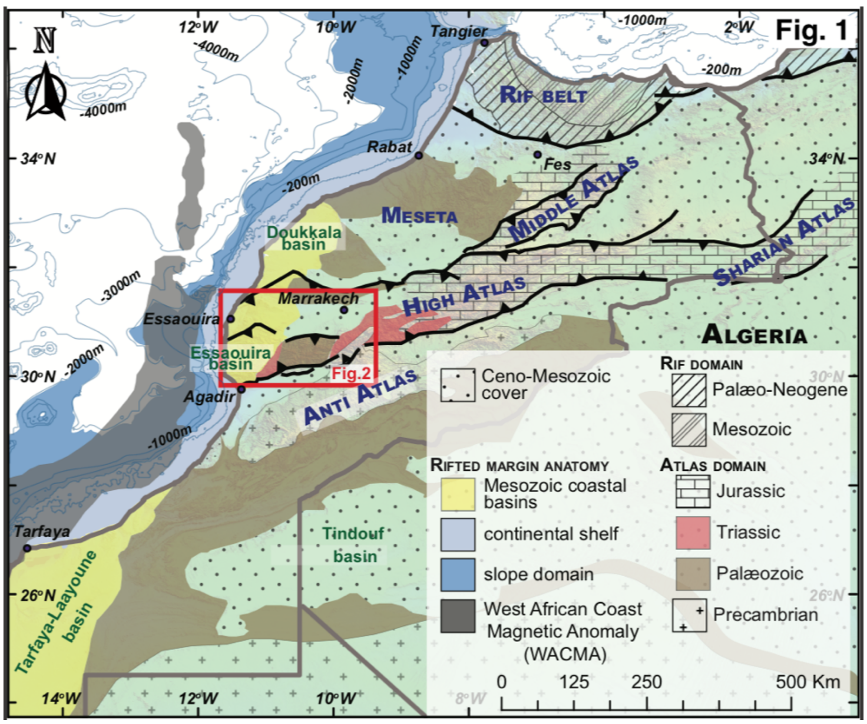

Fig. 1. Major tectono-sedimentary provinces of Western Morocco with the main Atlantic basins, modified after Gouiza 2011.

2 Geological background

The Essaouira Basin forms the western termination of the Moroccan High Atlas. It evolved as part of the Atlantic rift during Triassic to Early Jurassic times and as a proximal shallow-water platform of the Atlantic rifted margin since the Middle Jurassic (e.g., Hafid 2000). Later, during the Late Cretaceous to present-day convergence between Africa and Iberia/Europe, the Essaouira Basin in particular and the Atlas rift in general, experienced a N-S to NNW-SSE shortening and inversion leading to the build-up of the Atlas Mountains (e.g., Hafid et al. 2006; Hafid 2000; Piqué et al. 2002).

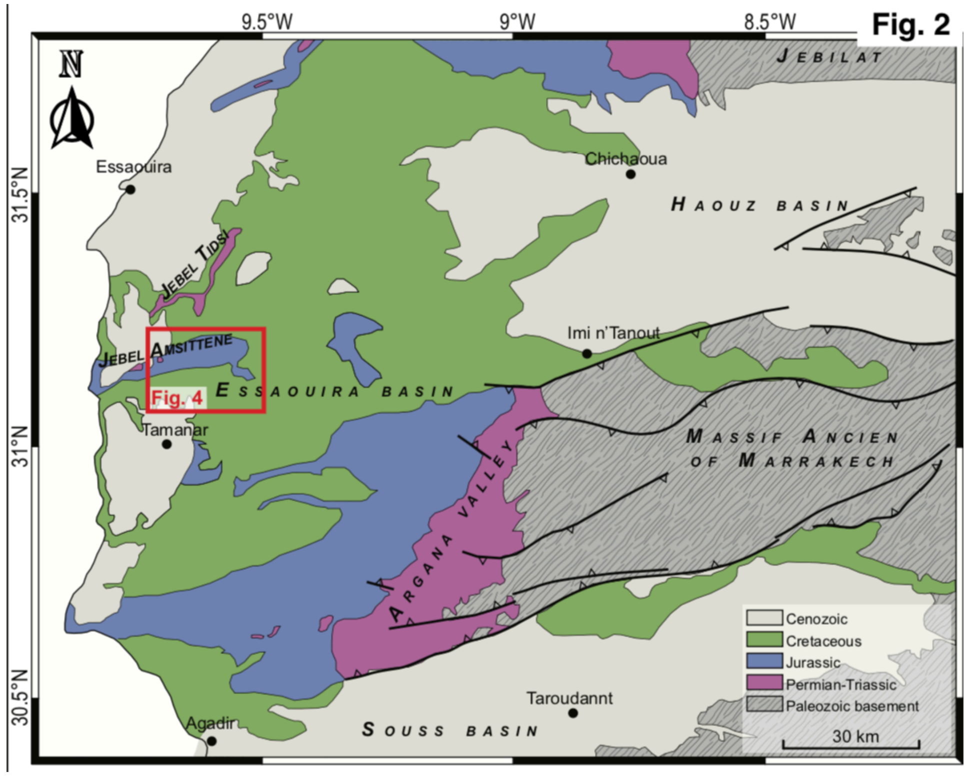

Fig. 2. Geological map of the western High Atlas (inverted Agadir continental margin basin), the southern part of the Essaouira Basin and the northern part of the Souss Basin. Simplified after Jadi, Bencheqroun, and Diouri (1970a,b), Ouzzani, Eyssautier, Marcais, Choubert and Fallot (1956), and Saadi (1982). From R. Zuhlke et al, 2004.

The extensional rift structures in the Essaouira Basin are grabens and half-grabens bounded by N-S to NNE-SSW normal faults and E-W transform faults (Hafid et al. 2006; Hafid 2000). These structures are filled by terrigenous red beds of Triassic age, unconformably overlain by an early Lower Jurassic evaporitic sag basin with widespread intercalations of basalt flows (Hafid et al. 2006). An early Pliensbachian unconformity, which is commonly considered to be the breakup unconformity, seals syn-rift sequences and structures (Medina 1995). Following continental breakup in the Central Atlantic, sedimentation became mostly marine in the Essaouira Basin, leading to deposition of the Middle Jurassic to Lower Cretaceous thick carbonate platform, with sandstone and shale interbeds, and the Upper Cretaceous to Neogene shale-dominated series, with intercalations of limestone beds (Hafid 2000). The shortening in the Atlas domain, which initiated in the Late Cretaceous and led to the formation of the Atlas fold-and-thrust belt (Frizon de Lamotte et al. 2000; Piqué et al. 2002; Teixell et al. 2003), is also believed to form salt-cored anticlines in the Essaouira Basin, with minor inversion of Triassic normal faults (Hafid et al. 2006).

The inversion and uplift of the Atlas belt is not the only major tectonic event that affected the Moroccan margin after the opening of the Central Atlantic Ocean. Analyses of low-temperature thermochronology document a major exhumation event that affected most of the Precambrian-Palaeozoic domains exposed to the east of the Atlantic margin (i.e. Meseta plateau, Jebilet, Massif Ancien of Marrakech, Anti-Atlas belt) during Late Jurassic-Early Cretaceous times (Ghorbal et al. 2008; Ghorbal 2009; Saddiqi et al. 2009; Ruiz et al. 2011; Oukassou et al. 2013; Sehrt 2014). The Palaeozoic basement highs bounding the Essaouira Basin, the Massif Ancien of Marrakech to the east and the Jebilet to the northeast, experienced km-scale exhumation during the Late Jurassic-Early Cretaceous (Ghorbal 2009; Saddiqi et al. 2009). Exhumation events are also documented along the margin in the Meseta plateau to the north (Ghorbal 2009; Saddiqi et al. 2009) and in the Anti-Atlas to the south (Malusà et al. 2007; Ruiz et al. 2011; Oukassou et al. 2013; Sehrt 2014; Gouiza et al. 2017; Charton et al. 2018). Regional exhumation occurred during the post-rift stage of the Central Atlantic Ocean, i.e. 30 to 50 Myr after lithospheric breakup between Morocco and Nova Scotia (Klitgord and Schouten 1986; Sahabi et al. 2004), and before the Atlas/Alpine contraction that gave rise to the Atlas and the Rif mountain belts (Frizon de Lamotte et al. 1991, 2008; Laville and Piqué 1992).

3 Fieldwork observations from Jbel Amsittene Anticline

Jbel Amsittene is a well-exposed salt-cored anticline that strikes ENE-WSW. It is located on the coastal plain of the W Moroccan Atlantic margin, in the northwest of the Essaouira Basin between the cities of Essaouira to the north and Agadir to the south (Figs 1 and 2).

The stratigraphy of Jbel Amssittene used in this study is based on Duffaud et al. (1966), Jaïdi et al, (1970) and Zühlke et al. (2004). The stratigraphic column shown in Fig. 3 is taken from the 1:100000 Geologic Map of the study area (Jaïdi et al. 1970), and shows an almost-continuous series of Upper Triassic to Lower Cretaceous rocks unconformably covered by Quaternary sediments in areas near the coast. The oldest formation, exposed in the core of the anticline, comprises Upper Triassic (T) terrigenous sandstones and evaporites. A stratigraphic gap marks an erosional event that occurred before the deposition of open marine rocks during the Early Jurassic (J0-J1). A gradual transition from floodplain to inner shelf environment, during the Middle Jurassic (J2-J3), resulted in a sedimentary change from predominantly siliciclastic sand to shallow marine carbonate. The Upper Jurassic (J4-J5) sediments are mainly shallow marine carbonates of inner shelf to lagoonal environment, although there remains some siliciclastic input. A change from inner shelf (J/C-C1-C2) to outer shelf environment occurred by the end of the Early Cretaceous (C3). Quaternary terrestrial colluviums and coastal deposits overlie the Mesozoic deposits (Fig. 3).

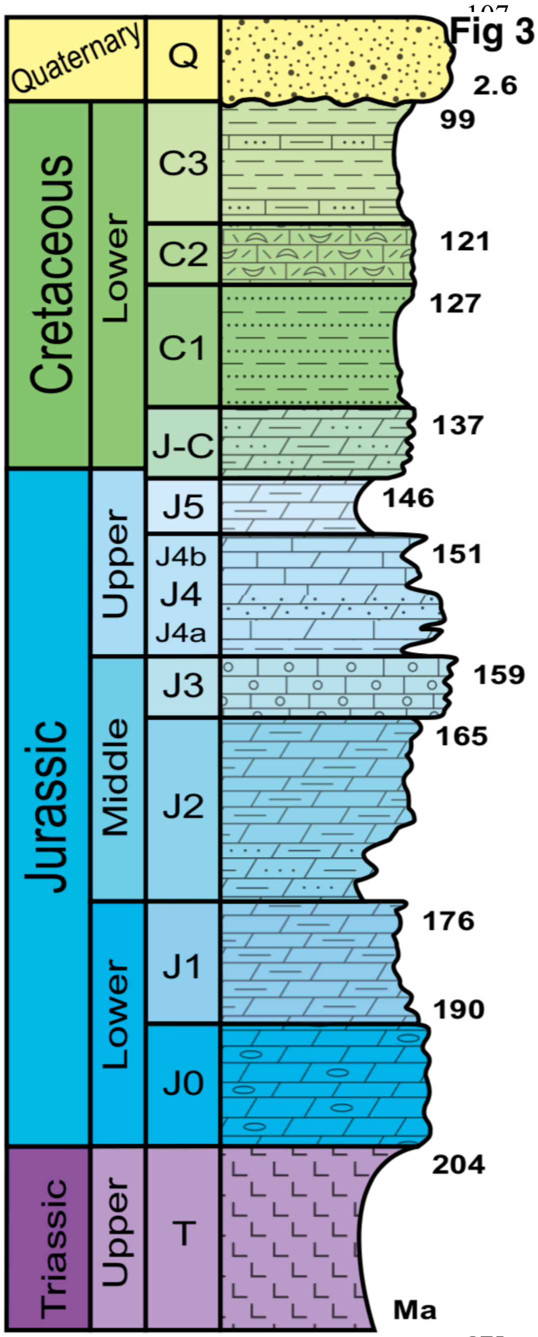

Fig. 3. Simplified chronostratigraphic and environmental column of the Jbel Amsittene area. Based on Hafid (2000), the Geological map of Tamanar from the Moroccan Geological Survey and Zlke et al. (2004).

To understand the tectonic history of the Jbel Amsittene Anticline, we performed a detailed structural fieldwork. Whenever possible, we have differentiated strain involving soft sediments depositing during the early post-rift of the Central Atlantic providing key information on the stress field during growth of the structures, especially in the Late Jurassic - Early Cretaceous, from observations of strain providing stress orientations of Alpine events, presumably in the Cenozoic. We show relevant and representative outcrops (Fig. 4) that summarize the main structural observations along three cross-sections.

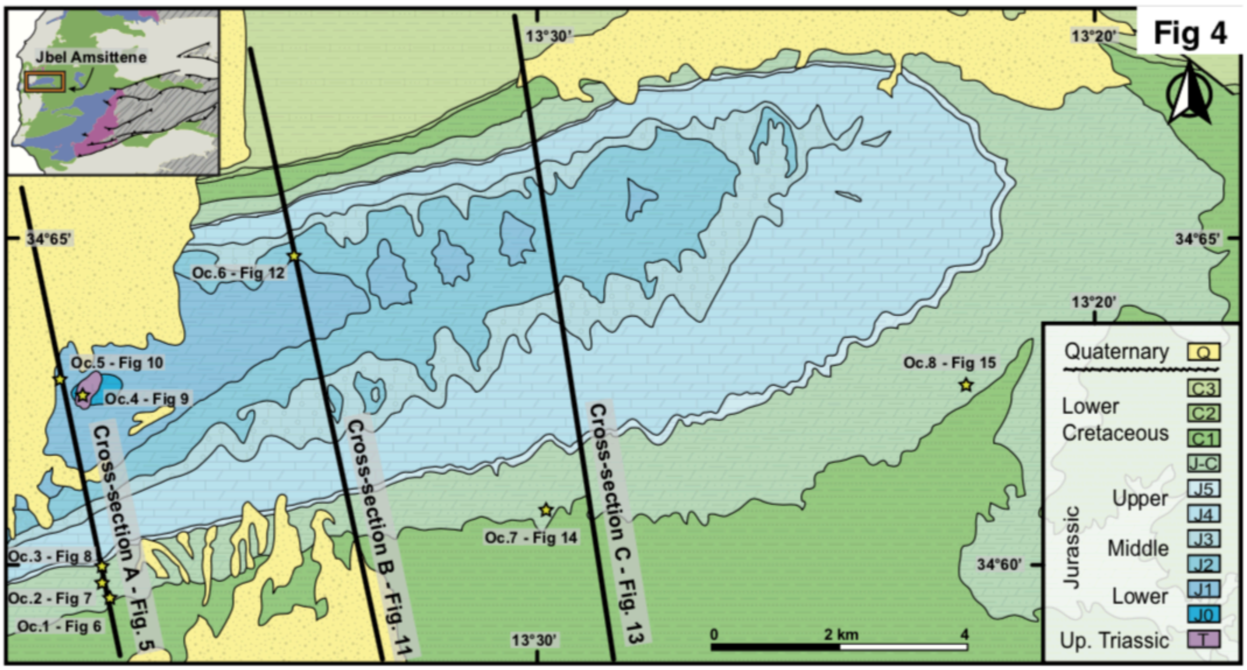

Fig. 4. Geological map of the Jbel Amsittene Anticline, showing the location of the main observations in the field and derived cross-sections that have been used to constrain the geological evolution of the area.

The geological cross sections, located roughly 4 km apart, run NNW-SSE across the anticline axis and were constrained by bed measurements and field observations. Cross-section A (Fig. 5) runs parallel (NNW-SSE) to a road-cut for most of its length, which results in the best rock exposures in the area. Jurassic and Cretaceous rocks outcrop in the south and central parts of the profile and are covered by the quaternary deposits in the northern region. Cross-section B (Fig. 11) is located ~4 km east of cross-section A and runs parallel to it. Cross-section B is often covered by vegetation and has poor accessibility with a small number of well-preserved outcrops. Cross-section C (Fig. 13) runs parallel to previous sections, and is located ~4 km east of cross-section B. We also describe two sections and an outcrop located farther east. Finally, we describe and recapitulate information relevant for the discussion in the form of along-strike and across-strike lateral variations, syn-sedimentary deformation, and a 3D thickness model.

3.1 Western profile: cross-section A

Lower Lower Cretaceous (C1) to lower Middle Jurassic (J2) layers dip south in most of the southern flank and change from horizontal to steeply north-dipping where the topography is the highest. North of the topographic high, layers dip south again and finally outcrop as overturned, prior to being covered by the Quaternary deposits in the northernmost area of the section. These outcropping Quaternary rocks prevent thickness comparison between most older units on both sides of the anticline, but those that could be compared show no thickness changes. The transition from horizontal to overturned layers is observed in the oldest Jurassic rocks exposed in this section (lowermost Jurassic, J1). The dip of the stratigraphic layers indicates a northward verging anticline with a tête-plongeante (plunging head) shape (sense Seguret 1972) in its central-northern sectors.

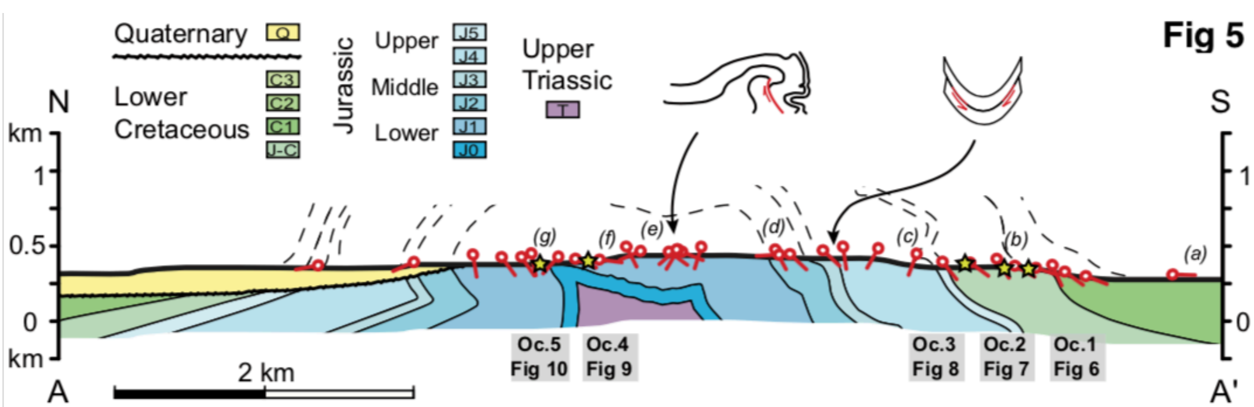

Fig. 5. Western profile: Cross-section A.

Lower Cretaceous rocks dip gently to the south (10˚-20˚) in the southernmost part of the southern flank ("a" in Fig. 5), and become steeper towards the north, reaching dips of ~80˚ at the highest point of the topography. Changes in dip are not constant and north dipping layers outcrop in the central sector of the southern flank (Fig. 5), within the middle and lower Upper Jurassic rocks (J4). Moving north, the dip of the layers locally changes in relation to secondary small-scale (tens of m) N-verging folds. In a local topographic flat (Fig. 5) there are three conjugate fault sets in the uppermost Upper Jurassic-lowermost Lower Cretaceous (J-C) limestones (Oc1; Fig. 6, Table I).

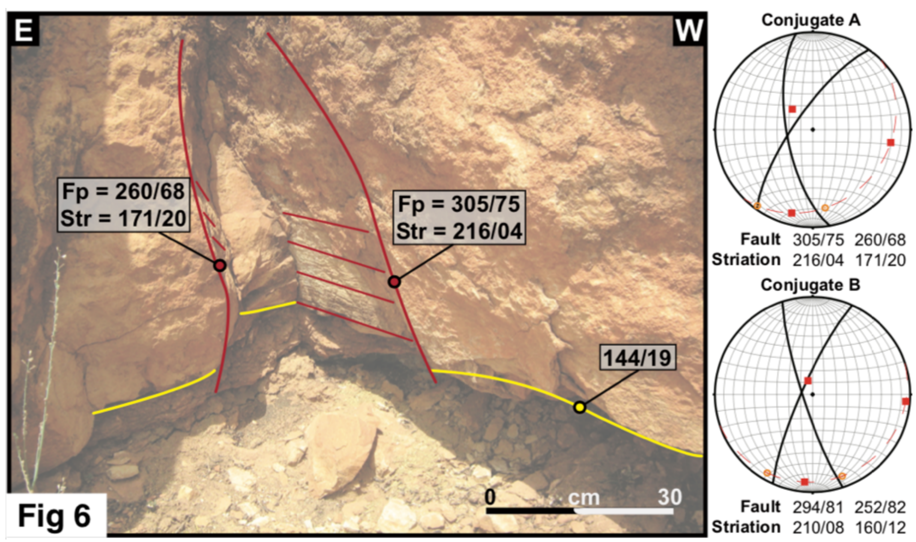

Fig. 6. Outcrop 1 (Oc.1). Conjugate sets and their stress directions, which indicate a north to south to north-northeast to south-southwest shortening.

Bedding	Present orientation			Orientation before tilting		
	σ_1	σ_2	σ_3	σ_1	σ_2	σ_3
144/19	010/09	256/68	103/20	014/22	208/67	106/02
144/19	183/01	282/81	093/09	005/13	171/76	274/03
146/28	203/28	344/56	103/18	195/11	031/79	286/03

Table I. Orientation of the main stresses derived from Out1 (Fig. 6).

The regional bedding dips gently to the SSE, and the three conjugate fault sets show clear striations of sub-horizontal to roughly S directions that we measure on the fault place as 216/04 and 171/20. The fault planes and associated striations are indicative of N-S to NNE-SSW maximum horizontal stresses in both non rotated rocks and rotated with respect to the regional bedding (to pre-tilt position). From this outcrop northwards, the strata dips start to increase and reach values up to ~55˚ toward the south ("b"; Fig. 5). Less than 50 m before the exposure of the lower Lower Cretaceous rocks (C1), a N-S-striking sub-vertical neptunian dyke of marine clastics cuts S-dipping strata (Oc2; Fig. 7). A few meters northwards, a syn-sedimentary N-verging ramp fold indicates soft sediment deformation (Oc3; Fig. 8). Whereas the conjugate fault sets in Oc.1 suggest no deformation took place before deposition of lowermost Lower Cretaceous – uppermost Upper Jurassic unit (J-C), the latter two synsedimentary structures (Oc2; Oc3) indicate NNW-SSE shortening during its deposition.

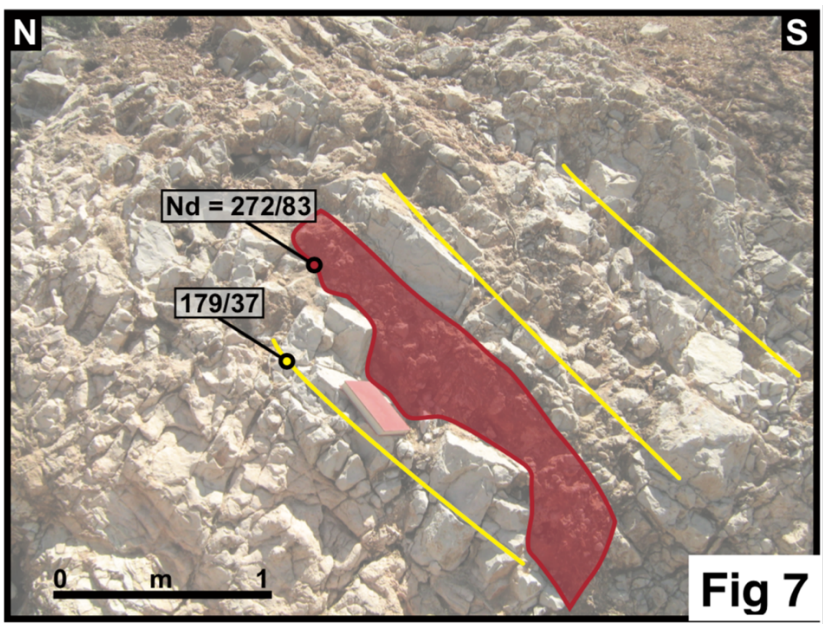

Fig. 7. Outcrop 2 (Oc.2). Neptunian dyke with a present position of 272/83. Assuming horizontal bedding at the moment of deposition, the neptunian dyke developed vertically, and suggests east-west extension.

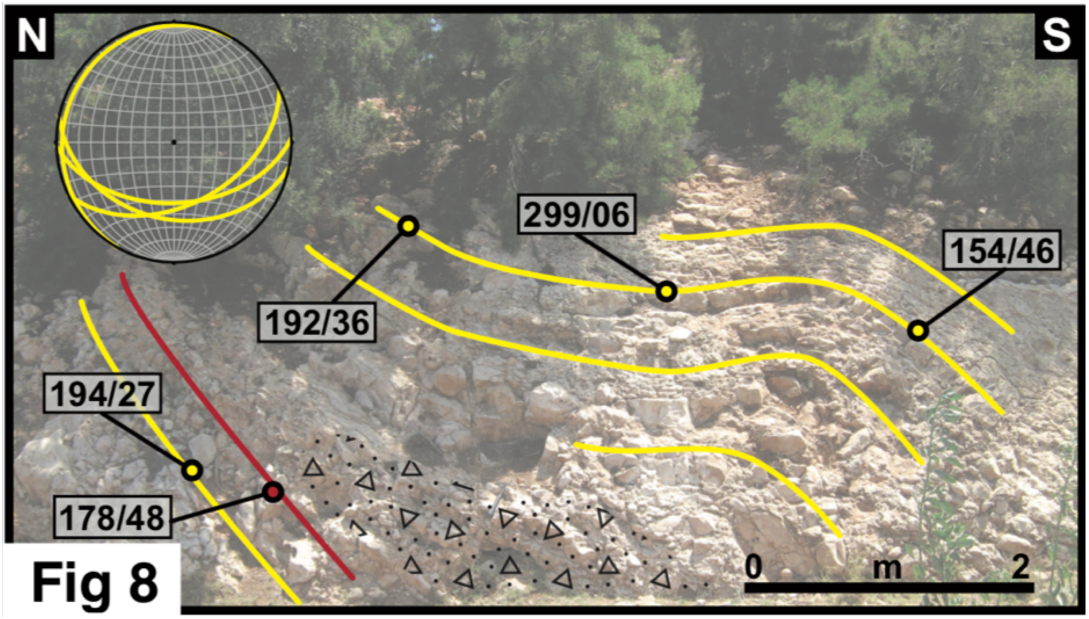

Fig. 8. Outcrop 3 (Oc.3). Folded and faulted soft sediments in a syn-sedimentary ramp fold, verging north, indicating shortening in a 160-340 direction during the 144-150 Ma (latest Jurassic).

Structures north of these outcrops seem to be exclusively related with the Alpine deformation phase. Approximately 200 m north of these outcrops, the Upper Jurassic layers (J5) are found dipping north ("c" in Fig. 5). For some 400 m, in the lower and middle Upper Jurassic rocks (J4), these steep and sub-vertical N-dipping overturned layers often alternate with areas of S dipping rocks with similar attitudes ("d"). Bedding-parallel flexural slip associated with Alpine deformation is common and related striations show a N-S slip direction. Northward, Middle Jurassic (J3-J2) strata dip consistently south until the highest topography of the profile is reached ("e"). North of the topographic high, the orientation of Lower Jurassic strata (J1) changes from subvertical (~80˚) to subhorizontal with a gentle S-dip within a distance of ca. 500 m (Fig. 5). Between the sub-vertical and sub-horizontal Lower Jurassic (J1) layers, S and N sub-vertical dipping strata alternate. Within this sector ("f" in Fig. 5), highly deformed structures appear, showing faulted and folded strata, m-folds, recumbent folds, fault-related-folds, and more complex features, with unclear or non-sequential vergence. More to the north the strike of the Lower Jurassic strata show no consistent trend for ~300 m, and outcrop as overturned (up to ~60˚) or S-dipping layers. At a similar latitude,

~300 m east off the section and roughly 5 km south of Smimou village, Upper Triassic evaporites (T) outcrop in a circular depression of approximately 1 km in diameter (Oc.4; Fig. 9). An intrusive contact is seen between the evaporites and the lowermost Jurassic unit (J1). The Lower Jurassic bedding dips away from the outcropping evaporites, from sub-vertical nearby to 25˚ farther away from them. The strike directions of these Jurassic rocks vary consistently around the salt, in an overall concentric configuration. The strike directions progressively change to the regional E−W to SW−NE trends 300-400 m away from the evaporites. Continuing north along the cross-section A, overturned strata become subvertical (80˚-85˚) (“g”) and finally N-dipping, before reaching the discordant sub-horizontal Quaternary (Q) rocks that cover most of the northern flank. In this area, a sequence of SSE-verging fault-propagation folds (Oc.5; Fig. 10) outcrops in the Lower Jurassic (J1), with axial planes indicating a SSE-NNW shortening direction (Fig. 10).

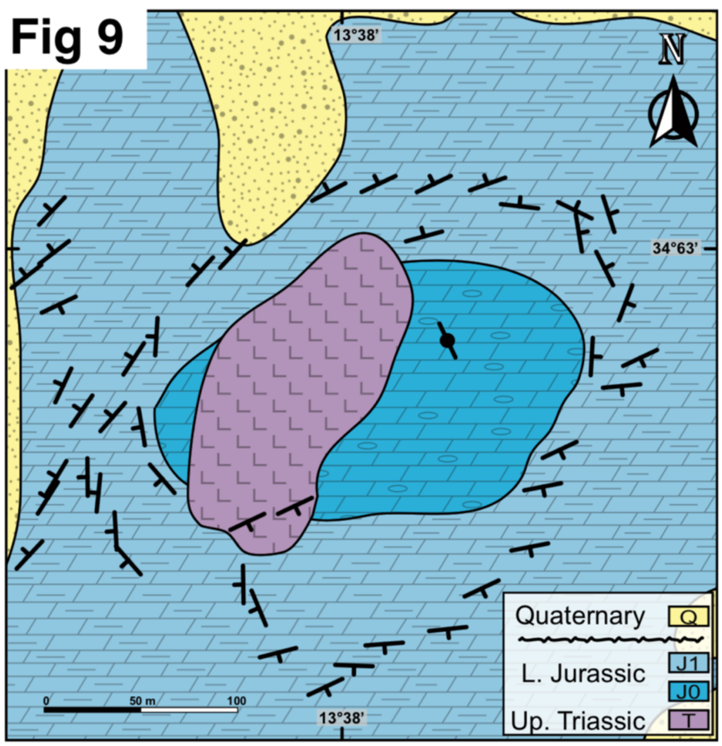

Fig. 9. Outcrop 4 (Oc.4). Map of the salt outcrop in the west and adjacent formations, showing the bedding strikes around the evaporitic body.

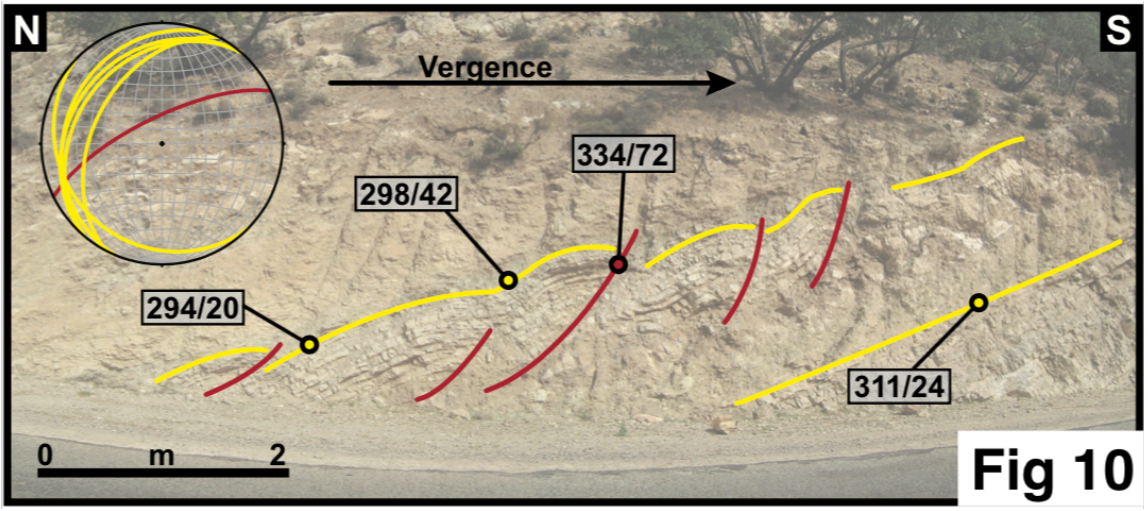

Fig. 10. Outcrop 5 (Oc.5). Reverse faults and folds with southeastern vergence, in outcrop situated less than 200 meters east of the outcropping salt (Fig. 9). Rocks in the outcrop are not affected by halokinesis, and show signs of compressional deformation. The orientation of the fault planes and the axial planes of the folds are similar and indicate NNW-SSE shortening.

3.2 Central profile: cross-section B

Gently south dipping lower Lower Cretaceous (C1) to lower Middle Jurassic (J2) layers outcrop from the southern side of the anticline until significantly north of the topographic high (Fig. 11). The oldest rocks seen in the section are Lower Jurassic (J1) and outcrop ~1,5 km north of the topographic high, in the core of the anticline. North of the hinge of the anticline there are steep north dipping layers of lower Middle Jurassic (J2) to Lower Cretaceous (C1) age. Some of these steep layers are overturned and dip south. Further north, the Lower Cretaceous strata (C2-C3) have gentle north dipping slopes. The uppermost Upper Jurassic to lower Lower Cretaceous (J-C to C1) rocks are significantly thinner in the northern (~350 m) than in the southern (>900 m) flank of the Jbel Amsittene (Fig. 11).

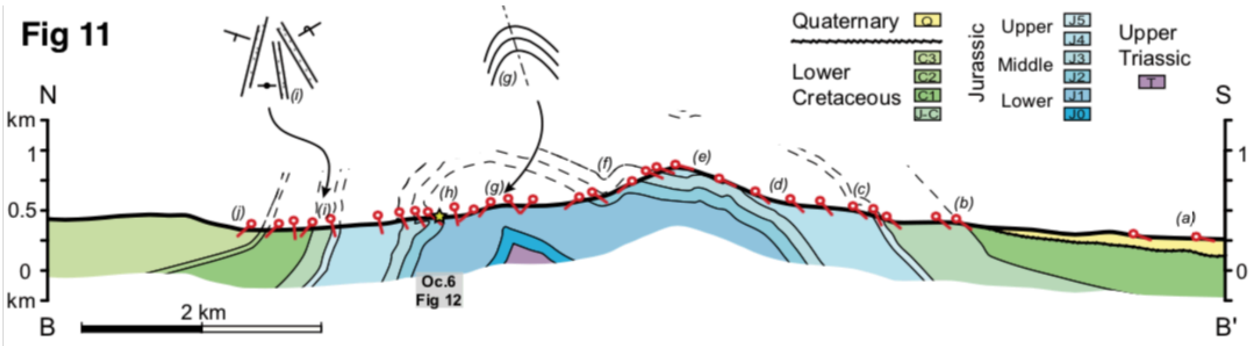

Fig. 11. Central profile: Cross-section B.

In the southernmost of cross-section B, Quaternary (Q) deposits cover Lower Cretaceous rocks (C1-C3) ("a" in Fig. 11). Northwards, the rocks of the uppermost Upper Jurassic to lower Lower Cretaceous (J-C to C1) outcrop with consistent dips of ~40° to the south ("b"). Upper Jurassic (J4-J5) layers have steeper dips that vary from ~40° to ~65° to the south ("c"). Moving north, the Middle Jurassic (J2-J3) layers gradually decrease in steepness from ~45° to ~35° to the south ("d") and become roughly parallel (10°-20° to the south) to the topography ("e") as they reach the topographic high.

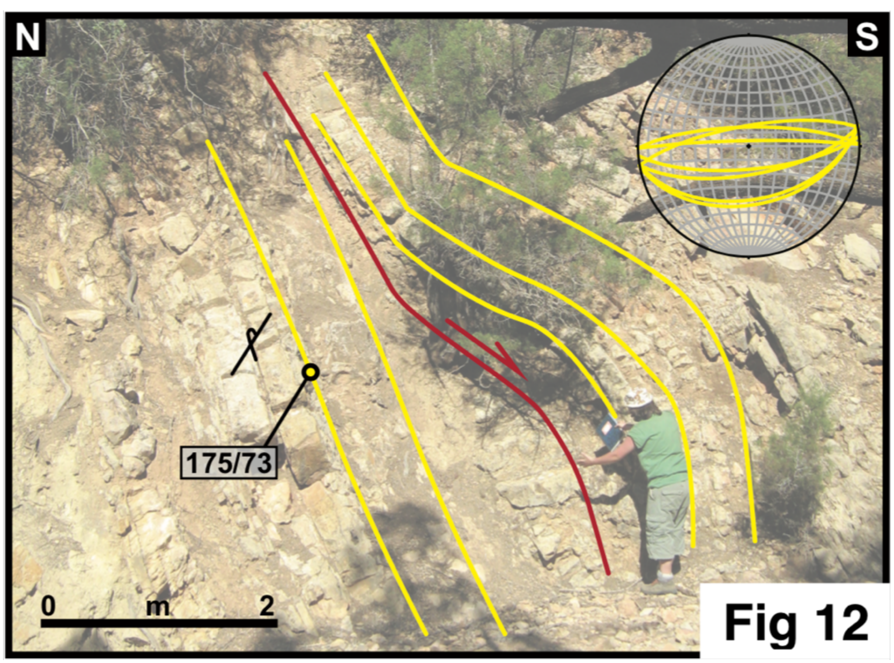

Fig. 12. Outcrop 6 (Oc.6). Underthrust in overturned strata, S_0 is 175/73. Fault-bend fold, with top to the south movement. The fold in the hanging wall has a fold axis of 085/06 and axial plane of 022/14.

Starting 300 m northwards of the topographic high, ~20° to 40° south dipping layers alternate with ~40° north dipping layers. This trend continues for ~400 m, and is seen also for part of the Lower Jurassic (J1) rocks ("f"). Layers are folded asymmetrically in this area until the northward dips become dominant ("g" in Fig. 11). Advancing farther north, these Lower Jurassic (J1) layers overturn and dip south again, for a distance of more than 900 m. Lower Middle Jurassic (J2) overturned layers outcrop showing the largest overturn along this profile (175°/73°) ("h"). These Jurassic rocks are locally underthrusted in a fault-bend fold structure that indicates top to the south motion (Oc.6; Fig. 12). The layers remain sub-vertical for around 1100 m, and gradually decrease in steepness, from ~85° to ~50° to the north, in the lowermost Cretaceous (J-C) unit ("i"). Toward the north, layers of the lowest Lower Cretaceous (C1) are sub-vertical again, while the middle Lower Cretaceous (C2) strata have shallower dips (40° N) ("j") that decrease gradually to 20° N when reaching the upper Lower Cretaceous (C3) rocks. Observations along the cross-section B show no evidence of synsedimentary deformation in the uppermost Upper Jurassic to lower Lower Cretaceous (J-C to C1) rocks but these units show a decrease of >500 m in thickness across the anticline strike.

3.3 Eastern profile: cross-section C

Cross-section C portrays a north vergent anticline with two hinges, showing a northern steep dipping flank and a southern shallow dipping flank (Fig. 13). The rocks exposed along this easternmost section are early Middle Jurassic (J2) to late Early Cretaceous (C3) of age. The thickness of the lowermost Cretaceous (J-C) formation varies from approximately 550 m on the southern flank to 400 m on the northern flank of the anticline, whereas the thicknesses of the Jurassic formations J2 to J5 are constant along the profile.

In cross-section C, the southern flank of the Jbel Amsittene Anticline is characterized in by south dipping sedimentary beds ("a" in Fig. 13), with subhorizontal Cretaceous rocks in its southernmost sector. Towards the north, older south-dipping rocks crop out. Within the lowermost Lower Cretaceous – uppermost Lower Jurassic formation (J-C), layer inclinations vary between approximately 30° and 80° to the south ("b"). Here, the layers are locally offset by cm to dm-scale reverse faults, which indicate N-S to NNE-SSW shortening coveal with sedimentation. Outcrop 7 (Oc. 7; Fig. 14) shows an example of these reverse faults. This SSW dipping fault has ~20 cm offset and terminates in the slumped overlying sediments that show soft deformation, indicating syn-sedimentary deformation during the early post-rift of the Central Atlantic.

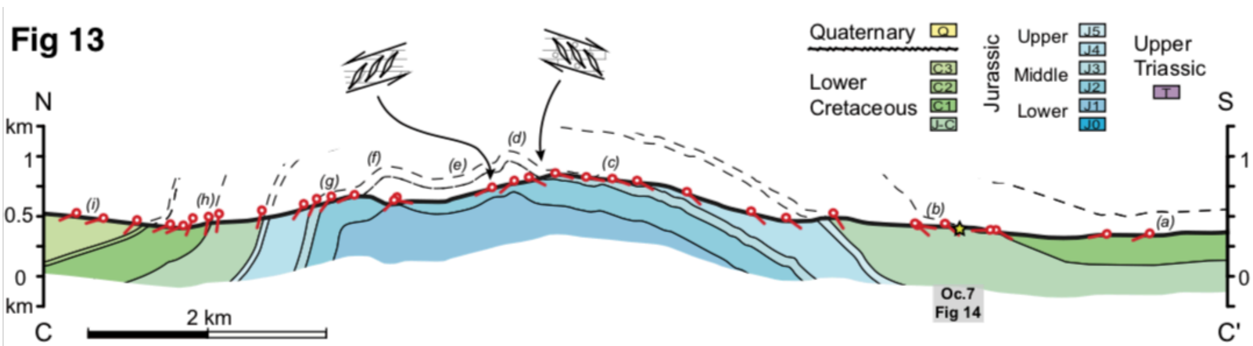

Fig. 13. Eastern profile: Cross-section C.

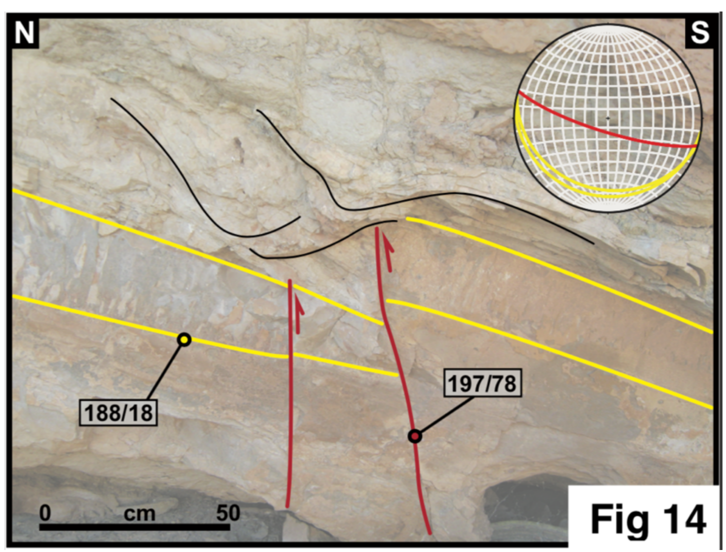

Fig. 14. Outcrop 7 (Oc.7). Inclined layers cut by synsedimentary faults. High-angle reverse faults transect a thick bank with an offset of ~20 cm. The reverse fault ends in the upper chaotic sedimentary layer that show soft sediment deformation. The timing of deformation is 146 to 137 Ma (J-C formation, lowermost Lower Cretaceous – uppermost Lower Jurassic).

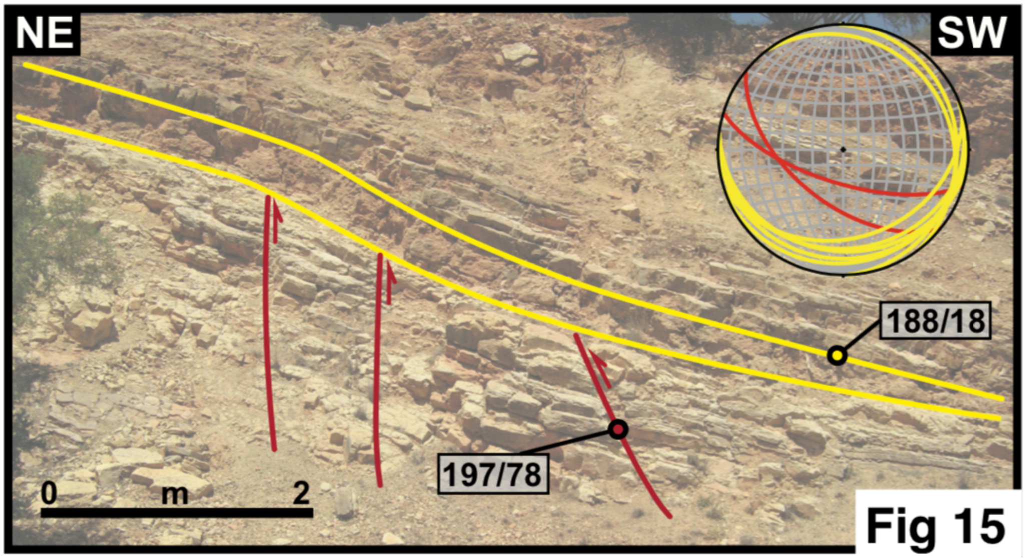

Fig. 15. Outcrop 8 (Oc.8). Approximately 30 m long wedge pinching out towards the south, overlaying faulted strata. The top to the northnortheast faults have reverse offsets of a few to tens of centimetres that do not continue in the wedge, indicating a shortening direction of SSW-NNE during the J-C formation, lowermost Lower Cretaceous – uppermost Lower Jurassic.

Outcrops farther north evidence deformation in relation to Alpine shortening. Towards the topographic high, the dip of the bedding gradually decreases from ~40° to 20° to the south, and upper Middle to middle Upper Jurassic (J3 – J4) rocks are exposed ("c"). Calcite-filled tension gashes are observed in several outcrops in and around the topographic high ("d" in Fig. 13). The veins are spaced by few cm, and show both top-to-the-north and top-to-the-south shear kinematics. The former occurs mostly to the south of the topographic high, and the latter is observed mainly to the north of the topographic high. Northwards, along a ~500 m sector, the beds are subhorizontal gently dipping to the north ("e"). Approximately 1 km farther north, beds dip to the south for ~100 m before dipping north again ("f") and lower Middle Jurassic (J2) rocks are exposed. In the second topographic high, where the second hinge plane of the anticline intersects the topography, the orientation of the bedding is 65° to the north ("g"). Between the second topographic high and the valley north of the Jbel Amsittene Anticline, successive upper Middle Jurassic (J3) to lower Lower Cretaceous (C1) strata are exposed steeply dipping north (60-80°) ("h"). North of the valley, Lower Cretaceous (C1 to C3) strata are exposed dipping ~10 to 20° northwards ("i").

3.4 Eastern sectors of the Jbel Amsittene and lateral variations

Other relevant structural observations were found eastwards of the above-described sections. The most relevant for the scope of this study outcrops ~5 km to the east of cross-section C, in the lowermost Cretaceous (J-C) limestones (Oc.8; Figs 4 and 15). This outcrop depicts a series of high angle reverse faults dipping SSW below a ~30 m long wedge that pinches out towards the S. The top-to-the-north faults show reverse offsets of few to tens of centimeters and slickenlines indicating SSW-NNE shortening direction. The fault tips lay within the overlying syn-tectonic strata, and indicate active shortening during the lowermost Cretaceous.

We reconstruct two other sections further east, where strain is more limited (Fig. 16). These sections are relatively similar in overall structure and geometry and change relevantly, albeit continuously, along the strike of the anticline. The eastern profiles depict a open and asymmetrical anticline with a gentle north vergence. In the eastern profiles, (i) the southern limb dips gently and persistently south, (ii) salt deformation is not noticeable, neither in the hinge nor elsewhere, and (iii) the northern limb shows north dips with no overturned strata. The anticline shows a well-confined hinge and its flanks dip more gently than their western continuations. Small-scale structures are rare and more open in character. The layers along the limbs alternate sectors of constant dip with others where they vary progressively. The western profiles present a tight structure and a clear north vergence. In the western profiles, (i) the southern limb of the anticline dips south, from gently to steep, with local dips to the north, (ii) distortion by diapirism is limited to near the hinge where the salt is outcropping, and (iii) the northern limb is frequently overturned and partly covered by Quaternary deposits. The western profiles show a topographic crest characterized by a north tête-plongeante geometry. Strain markers are numerous and strata often show relevant changes in dip direction over short horizontal distances.

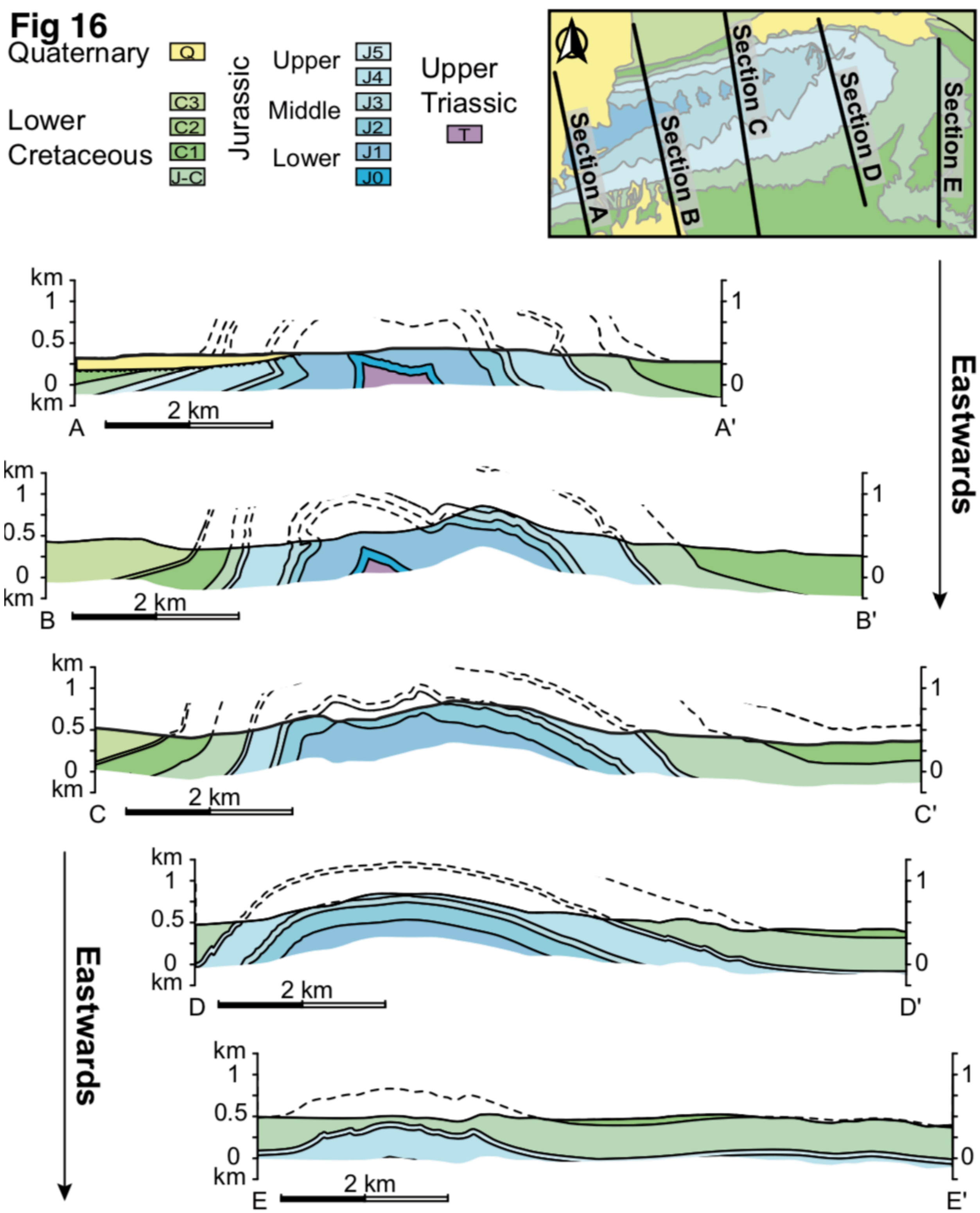

316

317 **Fig. 16.** Geological profiles from west to east.

3.5 Thickness changes along the Jbel Amsittene

To obtain thickness variations in the Jurassic formation, we put forward a 3D thickness model integrating remote sensing (horizon mapping) and structural data (dip data, geological cross sections) (Fig. 17). We use a "3 point-solver" plug-in for Google Earth™ to derive bed attitude from their contact with topography at three or more points (Bennison and Moseley 2003) and collect large-scale dip data at various locations around the anticline. We mapped horizons on DEM-coupled satellite images (Google Earth Pro™) to obtain spatial coordinates of well-exposed geological contacts, identified by the georeferenced geological map of Choubert (1965) and color changes in the imagery. We used the mapped horizons and the large-scale (tens of meters) dip data in geological cross-sections to derive a 3D model of continuous stratigraphic surfaces using *Gocad*'s *StructuralLab* tool. We then obtained true thickness maps by means of the *kine3d-1* tool that we extracted in the vicinity of mapped horizons using *Matlab*. Model resolution suggests a precision of ~20 m and hence lies below the thinnest stratigraphic units within the study area.

Lateral thickness maps reveal an along-strike change in the thickness of Jurassic rocks. Thickness variations in Figure 17 comprise the Lower Jurassic (J0, J1), Middle Jurassic (J2, J3), Upper Jurassic (J4, J5) along a clockwise profile from the northwestern to the southwestern fold flanks. Thickness decrease from the overturned northern flank, where maximum thicknesses exits, towards the east, with substantial decreases occurring at the point where the fold limbs change into NNW dipping beds. All formations follow this trend, that becomes less significant towards the Upper Jurassic (J4, J5). It is worth noticing, however, that modeling is less precise in overturned layers. In the southern limbs, towards the west, thicknesses in all formations increase progressively, albeit remaining below thicknesses of the northern limb (Fig. 17). Generally, thicknesses are never constant along strike for >5 km. Thickness at the eastern side yields around 40 to 50 m in the J3 and 140 m and 80 m for the J4, respectively. Sediments increase in thicknesses towards the southern limbs, yielding 140 to 200 m for the J3. This corresponds to a thickness increase of ~70- 75%. The J4a (Oxfordian) strongly increases from around 140 m to more than 300 m.

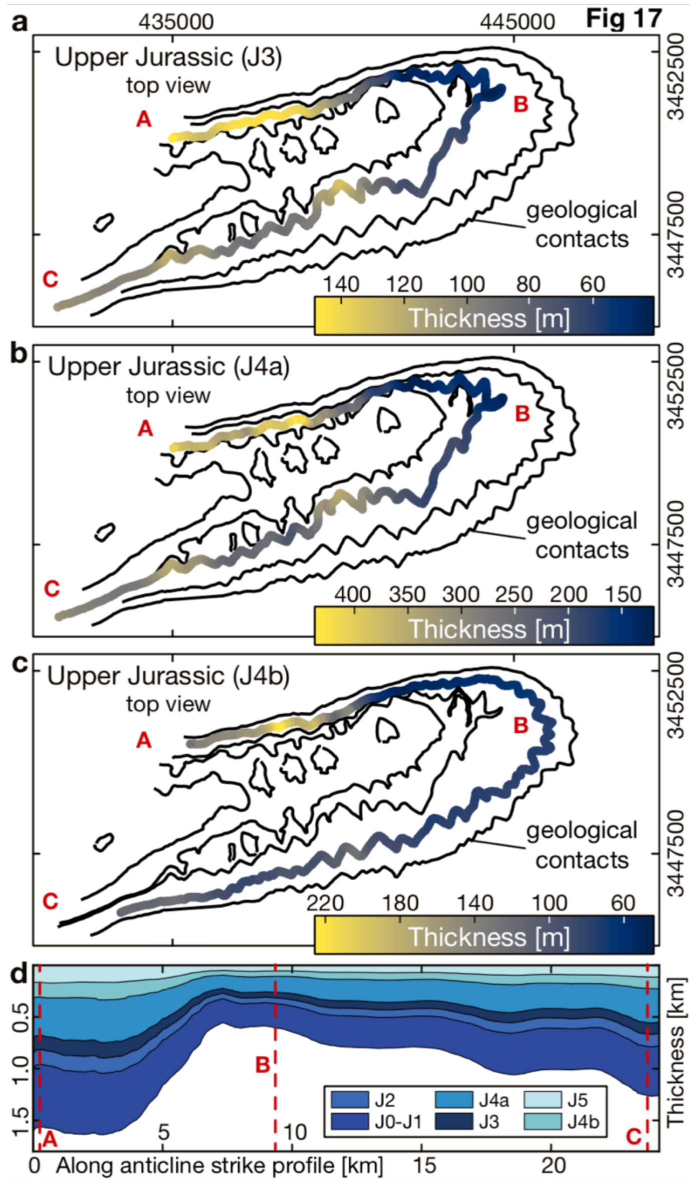

Fig. 17. a/b/c Model of thickness variations along contour likes of three Upper Jurassic sequences. **d** Modelled thickness variations of Jurassic rocks in a clockwise profile from the northwestern to the southwestern flank of the anticline.

We derive thickness in the upper Upper Jurassic - Lower Cretaceous sedimentary units (J-C, C1, and C2) from the attitude of beds within the units and along their contacts. We use this input to infer the planes of contact between the sedimentary units and calculate unit thicknesses by measuring orthogonally the distance between contacts. Although this approach is less accurate and lacks the along-strike coverage of the aforementioned thickness model, it provides a valid first-order signal on the across-strike variation of sedimentary thickness. These upper Upper Jurassic - Lower Cretaceous units (J-C, C1, and C2) decrease in thickness northwards across the strike of the Jbel Amsittene Anticline (Table II). As seen in cross-sections A and B (Figs. 5 and 11), formations J-C and C1 are up to ~350 m thinner in the northern flank with respect to the southern flank of the anticline (Table II). These values represent a minimum estimate, given that the upper boundary of C1 is on occasion outside the limits of our study area. Although unconstrained, our observations suggests that sedimentary thickness changes also affect also C2, and that no thickness changes affect the Lower Cretaceous C3 formation. These thickness variations are less obvious towards the east (Fig. 16).

	Formation J-C		Formation C1	
	N flank	S flank	N flank	S flank
Cross-section B	150m	500m	350m	500m
Cross-section C	400m	650m	350m	450m

Table II. Thickness changes between the northern and the southern flank of the Jbel Amsittene Anticline for formations J-C and C1.

4 Discussion

4.1 Key characteristics of the Jbel Amsittene Anticline

The Jbel Amsittene Anticline has a limited lateral extent and shows geometry changes along strike. In the west, the anticline manifests as a box anticline with a gentle north vergence within a broader area of deformation. The anticline continues west into the offshore, but seismic data show no folding ~10 km westwards off the coastline (Hafid, 2006). A tight tête-plongeante that the anticline has in the west smoothens and widens into an open fold (up to 40 km) and dims away eastward, as the anticline axial plane dips south and the fold axis plunges eastwards. Given the southward dip of the anticline axial plane, the oldest rocks at the anticline core locate to the north of the topographic high. Similarly, the eastward plunge of the anticline axis results in older rocks been exposed in the west.

Thickness variations have different trends in Jurassic and Early Cretaceous units. Jurassic units show a clear signal of westward decreasing thicknesses along strike (Fig. 17). Sharp thickness variations of up to

900 m occur between the northern flank and the eastern termination of the anticline, while thickness variations of ~600 m take place between the latter and the southern flank. A second-order signal across the anticline strike portrays a decrease in thicknesses towards the southern flank (Fig. 17). Uppermost Jurassic and Early Cretaceous units show the opposite trend. Sedimentary units J-C and C1 have thickness that decrease in up to 500 m northwards across the strike of the anticline, in turn decreasing eastwards some 150 m over short horizontal distances (Table II). Whereas thickness changes in Jurassic units seem unrelated with to a tectonic event, the latter units may relate with changes in shortening rates (see below).

Differential strain distribution along the anticline strike can be inferred for modern and antecedent forms of the Jbel Amsittene Anticline. We derive these along-strike strain changes from variations in the amount of shortening along the present anticline strike and from the number and size of outcrop-scale syn-sedimentary structures in the Upper Jurassic – lower Lower Cretaceous (J-C) formation (Table III). The western profile presents shortening values of ~1,6 km over a measured length of ~7,6 km, i.e., ~21% shortening. This shortening value remains almost constant in the central profile (~20 %), and decreases in the eastern profile (14,5 %). Farther east, in the easternmost section, we measured 0,2 km of shortening over a length of ~4,3 km, i.e. ~4,5 % shortening (Table III). Thus, strain decays along the Jbel Amsittene Anticline strike from its center to the east. Although most deformation and probably the observed eastward decay in shortening along the anticline strike relates to structure tightening during Alpine times, we infer a similar trend for the syn-depositional structures in the Upper Jurassic – lower Lower Cretaceous (J-C) formation. Most of such syn-depositional structures appear in the west of the anticline and are absent in rocks of the same age in the east and in the upper Lower Cretaceous (C3) rocks exposed in the northern part of the study area. This suggest that shortening that decreased eastwards resulted the growth of an anticline, albeit more open than at present, by the end of the Lower Cretaceous (C3).

	Deformed length (km)	Shortening (km)
Cross-section A	7,6	1,6
Cross-section B	9,5	2,1
Cross-section C	10,3	1,5
Cross-section D	9,1	0,6
Cross-section E	4,3	0,2

Table III. Decrease in amount of shortening to the east.

Syn-sedimentary deformation is common in outcrops of the uppermost Upper Jurassic-lowermost Lower Cretaceous limestones (J-C). Syn-sedimentary strain in these outcrops is expressed as neptunian dykes, fault-related folds and reverse faults affecting soft sediment (Figs. 7, 8, 14 & 15). Overall top-to-the-north steep reverse faults with tips that offset soft sediments by few to tens of centimeters (Figs. 8, 14 & 15) suggest N-S to NNE-SSW shortening. This observation can be potentially coupled with striae in nearby conjugate fault sets indicating NNW-SSE to NNE-SSW maximum horizontal stresses (Fig. 6). Similar evidence of syn-sedimentary shortening during deposition of the J-C unit can be found along the anticline strike. However, regional layer dips of the unit vary greatly (between approximately 30° and 80°), and evidence in other outcrops, such as the tête-plongeante or the overturned strata, are clear indications of later shortening of the Jbel Amsittene. Taken together, our data suggest that shortening during the early post-rift phase of the Central Atlantic initiated anticline growth of the Jbel Amsittene, and that the anticline further developed and tightened, presumably during the Alpine orogeny.

4.2 Models for the evolution the Jbel Amsittene Anticline

We put forward two potential models for the evolution of the Jbel Amsittene Anticline in Mesozoic times. We then discuss, on the basis of the evidence presented in this contribution, our preferred model for such initial anticline development, which was enhanced and partly overprinted in the Cenozoic. Comparative, detailed structural studies inclusive of similar onshore anticlines in the area are required to confidently discriminate among evolutionary models of the Jbel Amsittene anticline, and elucidate the underlying growth mechanism for equivalent structures in the Moroccan margin. Discrimination among different models in turn would have implications on the geodynamic causes controlling the anomalous vertical motions during the early post-rift phase along the African margin.

In a first scenario, we assume that the Triassic salt at the core of the present anticline is the driving force leading anticline growth already during the Early to Middle Jurassic. Halokinesis and salt tectonics are well expressed in the area (Hafid et al. 2006; Hafid 2000) and proposed to happen during this period in the Central High-Atlas (Saura et al. 2013). Although extensive diapirism exist offshore Morocco, no clear interpretation on timing and mechanism of salt mobilisation is available, and thus may occur in relation to different mechanisms than in the onshore (Neumaier et al. 2016). Still, vertical movements (Stets 1992; Bertotti and Gouiza 2012; Gouiza et al. 2017) could be linked to anticline fold growth and salt tectonics, such that a gravitational load is applied by the uplift of the High Atlas and a subsiding continental margin, creating a hydraulic head and consequent salt activation (Kluge 2016). The presence of salt in the anticline core and Jurassic thickness variations along the anticline that do not relate to the present structure are potential indicators for such salt tectonics scenario, although further evidence from nearby anticlines, such as the Imouzzer anticline, need to be found.

In a second scenario, the Jbel Amsittene Anticline initially developed by horizontal shortening in the latest Jurassic and earliest Cretaceous. Shortening during the Late Jurassic-Early Cretaceous marks an initial period of contraction and folding during the early post-rift phase that leads to the syn-tectonic growth of sedimentary wedges at anticline and outcrop scales (Figs. 8 & 11). Shortening started during latest Jurassic – earliest Cretaceous (J-C), continued during the deposition of the Lower Cretaceous unit (C1), and ended before the deposition of C3 unit. During this time, the Jbel Amsittene developed as open anticline that was probably asymmetrical along strike. The Triassic salt functions as a weak detachment facilitating accommodation of horizontal stresses leading to the partial inversion of pre-existing structures and initial anticline growth before Cenozoic tectonics (Hafid et al. 2006; Tari et al. 2003; Hafid 2006).

Evidence reported here favours early post-rift growth of the Jbel Amsittene by shortening. The shortening tectonics scenario is consistent with present of syn-sedimentary structures in the J-C unit and the existence of structures with clear vergence tens of meters away from the outcropping salt and well as with the limited strain (Figs. 7 to 10) near its contact. We similarly consider the lack of coherency in trend or scale of the salt with the overall anticline structure are also indicators of absence of halokinesis in the Jbel Amsittene during early post-rift of the Central Atlantic. Our observations imply that Triassic salts were mobilised during compression driven by horizontal tectonic forces, and the growth of associated structures occurs in relation to a blind thrusts rooted in the salts. The tête-plongeante structure towards the west and overturned layers at some sites indicate further shortening and anticline tightening during Alpine times. These geometries and their consistent changes along strike (Figs. 5, 11, 13 & 16) favour vertical anticline growth during two overprinting phases of shortening acting roughly in the N-S direction over growth by disruptive diapiric rise.

The ENE-WSW strike of the Jbel Amsittene Anticline is parallel to the strike of the major structures bounding the High Atlas belt (Fig. 2). These structures activated under a transtensional regime during the Triassic-Early Jurassic rifting, and defined several pull-apart basins where grabens and half-grabens, bounded by N- to NE-trending normal faults, were filled by terrigenous and evaporitic series (Piqué et al. 2002; Laville et al. 2004; Frizon de Lamotte 2005). In our attempt to reconstruct the evolution of the Jbel Amsittene through time, we hypothesize that the Jbel Amsittene Anticline formed in strata overlying a previous graben structure, which was bounded by an E-dipping normal fault to the east and an E-W transform fault to the north (Fig. 18). The presence and relative accommodation space expected from both these pre-existing structures could explain increasing Jurassic thicknesses westwards and northwards (Fig. 17), along and across anticline strike respectively. We interpret the upwards decreasing thickness in Upper Jurassic units (Fig. 17) as an indication that the aforementioned faults were nearly sealed by the end of the Late Jurassic. Subsequent Late Jurassic-Early Cretaceous folding of the Jbel Amsittene Anticline may have occurred by reactivation of the E-W structure as a blind thrust. This would result in thickness that increase towards the hanging-wall, i.e. southwards across the anticline and are thus opposite in trend with regards to those in the Jurassic units (Table II). Such blind thrust would be rooted in Triassic evaporites that act as a weak decollement layer between the basement and the overlying Mesozoic basin infill (Fig. 18). Therefore, most of the strain was localised in the depocentre of the Triassic salt found underneath the western part of the Jbel Amsittene and wedging out towards the east. This is coherent with eastwards decreasing strain observed for both the early post-rift and the Alpine shortening phases.

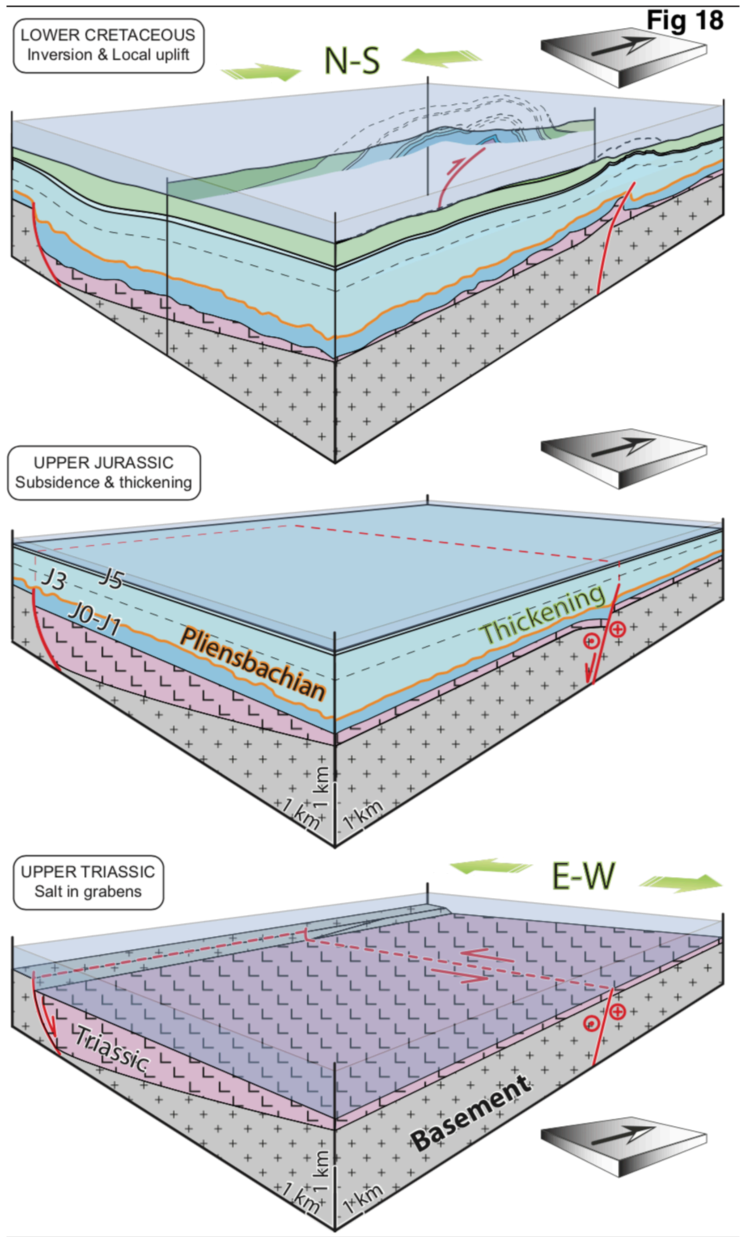

Fig. 18. Proposed evolutionary model of the Jbel Amsittene Anticline. In the last time-step we show the anticline with its finite geometry at present, which also results from Alpine tectonism.

4.3 Regional shortening during anticline growth

Observations from other areas within and nearby the Essaouira Basin suggest that the other salt structures present in the margin, may not have originally developed entirely during the Tertiary contraction. This is the case of the Tidsi Anticline and the Imi n'Tanout wedge in the Essaouira Basin, and the Dadès Valley in the Ouarzazate Basin. These structures may have formed similarly to the Jbel Amsittene Anticline, i.e. during an early post-rift shortening phase that reactivated inherited structures in assistance of the Triassic evaporitic rocks (Fig. 17). However, truncation of the basalt horizons by the Pliensbachian unconformity within certain structures also suggest the presence of earlier salt growth (Hafid et al. 2006).

The Tidsi Anticline, north of the Jbel Amsittene Anticline, was also thought to result from salt diapirism during the Late Cretaceous; the main arguments were the presence of growth strata documented in the Upper Cretaceous rocks coupled with the absence of tectonic indicators associated with these growth features (Amrhar 1995; Hafid 2006). While the relevance of diapirism in controlling the growth of the Tidsi Anticline during Late Cretaceous time is not unlikely, other older structures are observed in the area which document the existence of Early Cretaceous tectonic deformations hitherto neglected (Bertotti and Gouiza 2012). The best structures are visible along a >1 km long cliff in the southern part of the Tidsi Anticline where Triassic to Cretaceous sediments outcrop. A clear wedge described by Lower Cretaceous rocks opens southwards bounded on the southern side by steeper layers showing folded Early Lower Cretaceous beds along a WNW-ESE to NW-SE axis, that is parallel to the strike of the wedge. Strata geometry points to a NNE-ward vergence of the structure. Late Lower Cretaceous strata in the uppermost part of the outcrop are sub-horizontal, documenting the pre-Late Cretaceous age of deformation (Bertotti and Gouiza 2012). The tectonic nature of these structures is not only suggested by their overall geometry but is also proven by the fold vergence towards the core of the Tidsi Anticline, which is incompatible with a halokinetic origin.

To the east of Jbel Amsittene, the geometry of the post-rift portion of the Imi n'Tanout wedge prior to Alpine shortening was reconstructed coupling thickness measurements with structural field observations (Zühlke et al. 2004; Bertotti and Gouiza 2012). The post-rift strata show a gradual increase in thickness from NE to SW, reaching more than 3000 m towards the coastal areas and indicating that the Imi n'Tanout wedge opened along a NNW-SSE to NW-SE trending axis. Fieldwork observations in the Imi n'Tanout region reveal also the presence of two sets of shortening structures (Bertotti and Gouiza 2012). An older set oriented NW-SE to WNW-ESE is documented by syn-sedimentary structures that affect Middle Jurassic to Lower Cretaceous sediments to the south of the Imi n'Tanout line. At the outcrop-scale syn-depositional deformation is common in the Imi n'Tanout wedge and typically show folds and thrusts with a NW-SE trending axis. All these structures document Late Jurassic to Early Cretaceous NE-SW shortening approximately perpendicular to the axis of the Imi n'Tanout wedge suggesting that they developed within the same deformation regime. The younger set, oriented E-W to WSW-ENE, is found mainly in the Cretaceous sediments to the N of the Imi n'Tanout line and characterized by symmetrical to vergent folds. This set is conformal to the large-scale folds in the northern part of the Essaouira Basin that are related to the inversion of the Atlas system.

In the Ouarzazate foreland basin, located southeast of the Essaouira Basin and south of the central High Atlas (Fig. 1), strong evidences indicate a pre-Atlasic shortening event (Benvenuti et al. 2017). Observations from the Dadès Valley in the eastern Ouarzazate Basin indicate syn-tectonic angular and progressive unconformities within the Middle Jurassic to Lower Cretaceous stratigraphic units (Benvenuti et al. 2017). In addition, syn-sedimentary tectonic structures were also documented and suggest a first Middle Jurassic-Early Cretaceous NNE-SSW to NNW-SSE shortening and a later E-W shortening during the Late Cretaceous (Benvenuti et al. 2017).

4.4 Tectonic setting during anticline growth

The timing of the contractional structures observed in the Essaouira Basin coincides with major rearrangements in plate motions related to the opening of the South and North Atlantic Ocean. In fact, continental separation and accretion of oceanic crust in the South Atlantic (Torsvik et al. 2009), between SW Africa and South America, and in the North Atlantic (Knott et al. 1993; Tucholke et al. 2007), between North America and Eurasia, started in the Aptian-Albian time. The resulting counterclockwise rotation of Africa and the southward drifting of Iberia led to N-S compressive stresses within the African plate. At the same time, the ongoing oceanic accretion and mid-Atlantic ridge push in the Central Atlantic resulted in E-

W compressive stresses. We believe that Late Jurassic-Early Cretaceous shortening in the Essaouira Basin was driven by these N-S and E-W compressive stresses that reactivated the E-W and N-S syn-rift structures alike and initiated the subsequent salt movements onshore and offshore the Moroccan rifted margin (Hafid et al. 2006; Hafid 2000, 2006; Tari et al. 2003).

On the other hand, the spatial and temporal relation between these contractional structures and the regional uplift event that affected the NW African margin may suggest a common genetic process. Mantle processes like small-scale convection cells acting at the base of the mantle lithosphere cannot fully explain km-scale uplift of the crust during the early post-rift time their own, but if combined with intraplate stresses, the resulting uplift may be enhanced (Gouiza 2011).

5 Conclusion

We present structural and stratigraphic evidences demonstrating that the Jbel Amsittene is a N-verging fault-related anticline with its detachment plane in the Late Triassic evaporites. We have shown that the Jbel Amsittene (i) largely lack structures related to diapiric rise (only observable few hundred meters away from the outcropping evaporites), although recent literature promotes this mechanism; (ii) is an asymmetrical fault-propagation anticline with a steeply dipping northern, locally overturned, flank and a shallowly dipping southern flank; and (iii) underwent syn-sedimentary shortening during Late Jurassic-Early Cretaceous times.

The development of Jbel Amsittene was mainly driven by compressional tectonics and only partially the result of salt tectonics. The anticline formed during NNW-SSE shortening that initiated by the end of the Late Jurassic, potentially in the western part of the structure. Shortening resulted in syn-tectonic wedges at anticline and outcrop scale, in Late Jurassic and Early Cretaceous strata, while the effect of salt diapirism was restricted to a local area around the core of the anticline. The later inversion of the Atlas system in the Late Cretaceous and the Neogene caused the tightening of the anticline. Being one of many contemporaneous contractional structures reported in the Essaouira Basin and nearby basins linked to km-scale Middle Jurassic to Early Cretaceous exhumation event along the entire NW African margin, observations in the Jbel Amsittene Anticline suggest a tectonic evolution driven by intraplate stresses and deep mantle processes.

References

Amrhar M (1995) Évolution structurale du Haut Atlas occidental dans le cadre de l'ouverture de l'Atlantique centrale et de la collision Afrique--Europe: Structure, instabilités tectoniques et magmatisme. Thèse Doct. Etat, Univ. Cadi Ayyad, Marrakech

Bennison G, Moseley K (2003) An Introduction to Geological Structures and Maps 7ed

Benvenuti M, Moratti G, Algouti A (2017) Stratigraphic and structural revision of the Upper Mesozoic succession of the Dadès valley, eastern Ouarzazate Basin (Morocco). J Afr Earth Sci 135:54–71

Bertotti G, Gouiza M (2012) Post-rift vertical movements and horizontal deformations in the eastern margin of the Central Atlantic: Middle Jurassic to Early Cretaceous evolution of Morocco. Int J Earth Sci 101:2151–2165

Bonow JM, Japsen P, Green PF, et al (2009) Post-rift landscape development of north-east Brazil. Geological Survey of Denmark and Greenland Bulletin 17:81–84

Charton R, Bertotti G, Arantegui A, Bulot L (2018) The Sidi Ifni transect across the rifted margin of Morocco (Central Atlantic): Vertical movements constrained by low-temperature thermochronology. J Afr Earth Sci 141:22–32

Duffaud F, Brun L, Plauchut B (1966) Le bassin du Sud-Ouest marocain. Bassins sédimentaires du littoral Africain Publ Assoc Serv Géol Afric 1:5–26

Ellouz N, Patriat M, Gaulier J-M, et al (2003) From rifting to Alpine inversion: Mesozoic and Cenozoic subsidence history of some Moroccan basins. Sediment Geol 156:185–212

Frizon de Lamotte D (2005) About the Cenozoic inversion of the Atlas domain in North Africa. C R Geosci 337:475–476

Frizon de Lamotte D, Andrieux J, Guezou JC (1991) Cinematique des chevauchements neogenes dans l'Arc betico-rifain; discussion sur les modeles geodynamiques. Bull Soc Geol Fr 162:611–626

Frizon de Lamotte D, Saint Bezar B, Bracène R, Mercier E (2000) The two main steps of the Atlas building and geodynamics of the western Mediterranean. Tectonics 19:740–761

Frizon de Lamotte D, Zizi M, Missenard Y, et al (2008) The Atlas System. In: Michard A, Saddiqi O, Chalouan A, de Lamotte DF (eds) Continental Evolution: The Geology of Morocco. Springer Nature, Berlin Heidelberg, pp 133–202

Ghorbal B (2009) Mesozoic to Quaternary thermo-tectonic evolution of Morocco (NW Africa). Vrije Universiteit Amsterdam

Ghorbal B, Bertotti G, Foeken J, Andriessen P (2008) Unexpected Jurassic to Neogene vertical movements in "stable" parts of NW Africa revealed by low temperature geochronology. Terra Nova 20:355–363

Gouiza M (2011) Mesozoic Source-to-Sink Systems in NW Africa:: Geology of vertical movements during the birth and growth of the Moroccan rifted margin. Vrije Universiteit Amsterdam

Gouiza M, Bertotti G, Andriessen PAM Mesozoic and Cenozoic thermal history of the western Reguibat Shield (West African Craton). Terra Nova. doi: 10.1111/ter.12318

Gouiza M, Charton R, Bertotti G, et al (2017) Post-Variscan evolution of the Anti-Atlas belt of Morocco constrained from low-temperature geochronology. Int J Earth Sci 106:593–616

Hafid M (2000) Triassic–early Liassic extensional systems and their Tertiary inversion, Essaouira Basin (Morocco). Mar Pet Geol 17:409–429

Hafid M (2006) Styles structuraux du Haut Atlas de Cap Tafelney et de la partie septentrionale du Haut Atlas occidental: tectonique salifère et relation entre l'Atlas et l'Atlantique. Notes Mém Serv Géol Maroc 465:172

Hafid M, Zizi M, Bally AW, Ait Salem A (2006) Structural styles of the western onshore and offshore termination of the High Atlas, Morocco. C R Geosci 338:50–64

Jaïdi S, Bencheqroun A, Diouri M (1970) Carte Géologique du Maroc 1:100 000, Feuille Tamanar. Not Mém Serv Géol Maroc 201:

Japsen P, Bonow JM, Green PF, et al (2006) Elevated, passive continental margins: Long-term highs or Neogene uplifts? New evidence from West Greenland. Earth Planet Sci Lett 248:330–339

Japsen P, Bonow JM, Green PF, et al (2009) Formation, uplift and dissection of planation surfaces at passive continental margins – a new approach. Earth Surf Processes Landforms 34:683–699

Japsen P, Chalmers JA (2000) Neogene uplift and tectonics around the North Atlantic: overview. Glob Planet Change 24:165–173

Klitgord KD, Schouten H (1986) Plate kinematics of the central Atlantic. The Geology of North America 1000:351–378

Kluge C (2016) A Structural Modeling Approach on Timing & Evolution of Mesozoic Anticlines in the Western High Atlas, Morocco

Knott SD, Burchell MT, Jolley EJ, Fraser AJ (1993) Mesozoic to Cenozoic plate reconstructions of the North Atlantic and hydrocarbon plays of the Atlantic margins. In: Petroleum Geology of Northwest Europe: Proceedings of the 4th Conference. Geological Society of London, pp 953–974

Laville E, Piqué A (1992) Jurassic penetrative deformation and Cenozoic uplift in the Central High Atlas (Morocco): A tectonic model. structural and orogenic inversions. Geol Rundsch 81:157–170

Laville E, Pique A, Amrhar M, Charroud M (2004) A restatement of the Mesozoic Atlasic Rifting (Morocco). J Afr Earth Sci 38:145–153

Leprêtre R, Missenard Y, Barbarand J, et al (2015) Postrift history of the eastern central Atlantic passive margin: Insights from the Saharan region of South Morocco. J Geophys Res [Solid Earth] 120:2014JB011549

Le Roy P, Piqué A (2001) Triassic–Liassic Western Moroccan synrift basins in relation to the Central Atlantic opening. Mar Geol 172:359–381

Malusà MG, Polino R, Feroni AC, et al (2007) Post-Variscan tectonics in eastern Anti-Atlas (Morocco). Terra Nova 19:481–489

Medina F (1995) Syn- and postrift evolution of the El Jadida – Agadir basin (Morocco): constraints for the rifting models of the central Atlantic. Can J Earth Sci 32:1273–1291

Neumaier M, Back S, Littke R, et al (2016) Late Cretaceous to Cenozoic geodynamic evolution of the Atlantic margin offshore Essaouira (Morocco). Basin Res 28:712–730

Oukassou M, Saddiqi O, Barbarand J, et al (2013) Post-Variscan exhumation of the Central Anti-Atlas (Morocco) constrained by zircon and apatite fission-track thermochronology. Terra Nova 25:151–159

Peulvast J-P, Claudino Sales V, Bétard F, Gunnell Y (2008) Low post-Cenomanian denudation depths across the Brazilian Northeast: Implications for long-term landscape evolution at a transform continental margin. Glob Planet Change 62:39–60

Piqué A, Le Roy P, Amrhar M (1998) Transtensive synsedimentary tectonics associated with ocean opening: the Essaouira–Agadir segment of the Moroccan Atlantic margin. J Geol Soc London 155:913–928

Piqué A, Tricart P, Guiraud R, et al (2002) The Mesozoic-Cenozoic Atlas belt (North Africa): an overview. Geodin Acta 15:185–208

Ruiz G, Sebti S, Negro F, et al (2011) From central Atlantic continental rift to Neogene uplift--western Anti-Atlas (Morocco). Terra Nova 23:35–41

Saddiqi O, El Haimer F-Z, Michard A, et al (2009) Apatite fission-track analyses on basement granites from south-western Meseta, Morocco: Paleogeographic implications and interpretation of AFT age discrepancies. Tectonophysics 475:29–37

Sahabi M, Aslanian D, Olivet J-L (2004) Un nouveau point de départ pour l'histoire de l'Atlantique central. C R Geosci 336:1041–1052

Saura E, Vergés J, Martín-Martín JD, et al (2013) Syn- to post-rift diapirism and minibasins of the Central High Atlas (Morocco): the changing face of a mountain belt. J Geol Soc London 171:97–105

Seguret M (1972) Étude tectonique des nappes et séries décollées de la partie centrale des Pyrénées. Thesis. Science Univ. Montpellier

Sehrt M (2014) Variscan to Neogene long-term landscape evolution at the Moroccan passive continental margin (Tarfaya Basin and western Anti-Atlas). Heidelberg

Stets J (1992) Mid-Jurassic events in the Western High Atlas (Morocco). Geol Rundsch 81:69–84

Tari G, Molnar J, Ashton P (2003) Examples of salt tectonics from West Africa: a comparative approach. Geological Society, London, Special Publications 207:85–104

Teixell A, Arboleya M-L, Julivert M, Charroud M (2003) Tectonic shortening and topography in the central High Atlas (Morocco). Tectonics 22:1051

Torsvik TH, Rousse S, Labails C, Smethurst MA (2009) A new scheme for the opening of the South Atlantic Ocean and the dissection of an Aptian salt basin. Geophys J Int 177:1315–1333

Tucholke BE, Sawyer DS, Sibuet J-C (2007) Breakup of the Newfoundland–Iberia rift. Geological Society, London, Special Publications 282:9–46

Zühlke R, Bouaouda M-S, Ouajhain B, et al (2004) Quantitative Meso-/Cenozoic development of the eastern Central Atlantic continental shelf, western High Atlas, Morocco. Mar Pet Geol 21:225–276